Velocity fluctuations and Johnson noise in quantum wires: the effect of phonon confinement

1999 J. Phys.: Condens. Matter 11 3697

(http://iopscience.iop.org/0953-8984/11/18/306)

J. Phys.: Condens. Matter **11** (1999) 3697–3709. Printed in the UK PII: S0953-8984(99)00114-9

Velocity fluctuations and Johnson noise in quantum wires: the effect of phonon confinement

A Svizhenko†, S Bandyopadhyay† and M A Stroscio‡

† Department of Electrical Engineering, University of Nebraska, Lincoln, NE 68588, USA
‡ US Army Research Office, PO Box 12211, Research Triangle Park, NC 27709, USA

Received 21 December 1998, in final form 12 February 1999

Abstract. We have theoretically studied electron velocity fluctuations and the resulting Johnson (thermal) noise in a free-standing GaAs quantum wire at low and intermediate driving electric fields. One-dimensional confinements of electrons and phonons have been taken into account. Acoustic phonon confinement introduces infrared frequency peaks in the noise power spectrum which are an unmistakable signature of phonon confinement and provide an experimental 'handle' to use in assessing the importance of such confinement. Phonon confinement also suppresses the dc component of the noise spectral density (and the hot-carrier diffusivity) by several orders of magnitude. When a transverse magnetic field is applied to the quantum wire, it introduces three remarkable features: (i) it reduces the temporal decay rate of the velocity autocorrelation function and increases the dc component of diffusivity, (ii) it promotes prolonged and persistent oscillations in the velocity autocorrelation function which is indicative of a long memory of the electron ensemble, and finally (iii) it red-shifts the peaks in the noise power spectrum by increasing the length of an electron's trajectory in momentum space between two successive phonon scattering events.

1. Introduction

There is significant current interest in the application of quasi-one-dimensional semiconductor structures for high-speed and low-noise electronic devices such as quantum-wire field-effect transistors (QWFET). Such devices are expected to exhibit high transconductance, bandwidth and unity-gain frequency as a result of the enhancement of carrier mobility accruing from a constriction of the phase space for scattering. It is however not clear as to whether the same constriction necessarily leads to a reduction of the thermal (Johnson) noise as well. The purpose of this paper is to address this issue and investigate pertinent characteristics of Johnson noise in quantum wires.

Johnson noise in a solid is caused by fluctuations in the velocity of current carriers (electrons or holes) interacting with scatterers. It is thus expected that strong confinement of both electrons and phonons (the major scatterers) may have a significant effect on velocity fluctuations and the noise power spectrum. In this paper, we have studied velocity fluctuations in a free-standing GaAs quantum wire using a Monte Carlo simulation. Both electron and phonon confinements have been taken into account rigorously [1, 2]. In the past, similar studies [3] took into account electron confinement, but not phonon confinement. We found that phonon confinement is extremely important and leaves a strong signature in the noise power spectrum, as well as the temporal decay characteristics of the velocity autocorrelation function. In fact, measurement of the noise power spectrum offers a convenient tool for assessing

0953-8984/99/183697+13$19.50

experimentally the presence and importance of phonon confinement effects in quasi-one-dimensional structures. Moreover, acoustic phonon confinement decreases the dc component of the noise spectral density (and hence the carrier diffusivity) by *three to five* orders of magnitude and this in itself has important device implications.

Finally, we have investigated the effect of an external magnetic field on velocity fluctuations (and noise) since a magnetic field is known to strongly suppress carrier back-scattering events [5] and produce other effects associated with modifications of the carrier dispersion relation. We found that a magnetic field introduces additional features which depend strongly on whether phonon confinement is taken into account or not. For instance, a bulk phonon model predicts that diffusivity will decrease in a magnetic field whereas the confined phonon model reveals that the opposite is true. We also found that the dc component of the diffusion coefficient calculated from the dc component of the noise spectral density cannot be related to the mobility and carrier temperature by the Einstein relation. This is not surprising given the dominance of hot-electron effects which invalidate the Einstein relation and the existence of non-Markovian scattering processes which affect the usual relationship between the noise spectral density and the carrier diffusivity.

This paper is organized as follows. In the next section, we briefly describe our theoretical approach and the Monte Carlo simulator. This is followed by results and discussion. The last section details our conclusions.

2. Theory

We will calculate the temporal characteristics of the velocity autocorrelation function and Johnson noise power spectrum in a free-standing GaAs quantum wire of rectangular cross-section. An electric field is applied along the length of the wire to induce carrier transport and an external magnetic field is applied in a transverse direction parallel to the thickness dimension as shown in the inset of figure 1.

There is a sequence of steps in the calculation. We first solve the Schrödinger equation in the quantum wire (with only the transverse magnetic field present) to obtain the wave functions and the energy dispersion relations of the confined hybrid magnetoelectric states of electrons [6]. Next, the confined acoustic phonon normal-mode amplitudes and the dispersion relations of up to the twenty lowest-energy phonon branches (the so-called 'width' and 'thickness' modes) are found by solving the elasticity equation for the quantum wire numerically [2]. These branches span an energy range of up to $10\,kT$ (T = lattice temperature); as a result, higher phonon branches can be neglected since their occupation probabilities are extremely small. From the electron and phonon dispersion relations, we have calculated the joint electron–phonon density of states and hence the electron–phonon scattering rates based on Fermi's Golden Rule. These rates are then used in a Monte Carlo simulator to simulate Boltzmann transport and obtain an electron ensemble's average velocity as a function of time. From these data, we calculate the temporal decay of the velocity autocorrelation function in the presence of a driving electric field.

The Monte Carlo simulator is a modified code for quantum wires. The basic algorithm is described in references [3, 7–9] and it was modified to account for the complications associated with confined acoustic phonon scattering in a magnetic field. When acoustic phonons are confined, we have to determine the final state of an electron after a scattering event based on the initial energy of the electron, the initial and final magnetoelectric subbands occupied, the type of phonon mode (width or thickness) that mediated the scattering process, the phonon branch involved, and the type of the scattering process (forward absorption, backward absorption, forward emission, or backward emission). This requires an intensive search procedure which

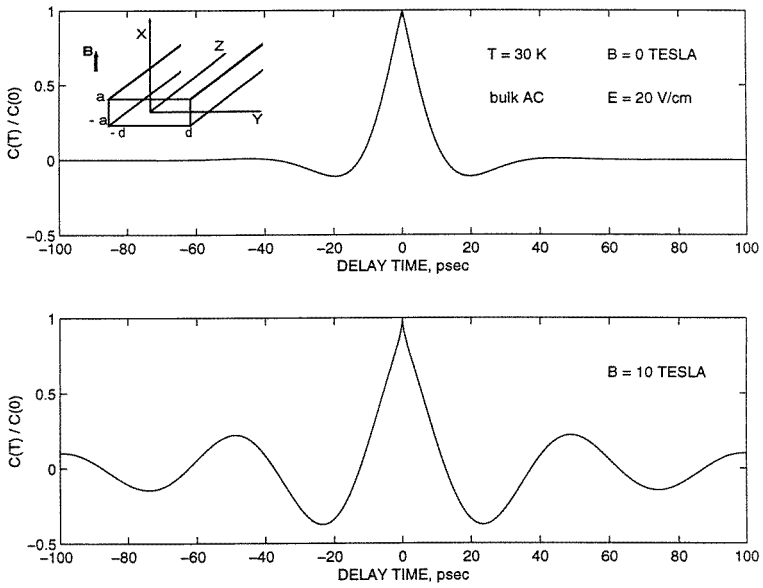

Figure 1. Temporal evolution of the velocity autocorrelation function at magnetic flux densities of 0 T (upper panel) and 10 T (lower panel). The driving electric field is 20 V cm^{-1}, the lattice temperature is 30 K, and the electron temperature is 108 K. A bulk acoustic phonon model has been assumed. The inset shows the geometry of the quantum wire and the orientations of the electric and magnetic fields.

is implemented through a Von Neumann technique [3] and a rejection algorithm. We collect velocity statistics after the steady state is achieved by using a uniform sampling in time.

The velocity autocorrelation function is defined as

$$C(T) = \langle \delta v(t)\, \delta v(t+T) \rangle \tag{1}$$

where $\delta v = v(t) - v_d$ (with $v(t)$ being the instantaneous carrier velocity at an instant of time t and v_d the steady-state (ensemble-average) drift velocity). The noise spectral density is obtained by evaluating the cosine transform of the autocorrelation function (the Wiener–Kintchine theorem):

$$S(f) = 2\int_0^\infty \mathrm{d}T\ \cos(2\pi f T) C(T) \tag{2}$$

and it is usually related to the dc component of the diffusivity $D(0)$ according to

$$S(f) = \frac{4D(0)}{1 + (2\pi f \tau_m)^2} \tag{3}$$

where τ_m is the ensemble-average momentum relaxation time. The validity of equation (3) is predicated on the assumption that velocity fluctuations decay *exponentially* in time with a characteristic momentum relaxation time τ_m. This is evidently not a good assumption since our scattering processes (acoustic and optical phonon scattering) are non-Markovian in that they are neither elastic nor isotropic. For such processes, a unique relaxation time cannot be defined [4]. Hence, equation (3) is suspect. In this paper, we will nonetheless calculate an 'effective' diffusion coefficient from equation (3) and show that it differs significantly from the Einstein diffusivity.

3. Results and discussion

We consider a GaAs free-standing quantum wire of width 300 Å and thickness 40 Å. Free-standing wires are now routinely fabricated using a variety of simple techniques such as impregnating naturally occurring 60 Å diameter channels in chrysotile asbestos with a molten semiconductor [13]. Carbon nanotubes are another example of free-standing wires. The routine availability of such systems has fuelled a commensurately increased interest in their transport properties.

We have studied electron transport using Monte Carlo simulation of carrier dynamics. The Monte Carlo simulation was carried out with an ensemble of 1000 particles at a lattice temperature of 30 K and magnetic flux densities of 0 and 10 T. The number of particles is more than sufficient to make the quantities in equations (1)–(3) independent of the ensemble size. The simulations were carried out at two different electric field strengths: a low field of 20 V cm^{-1} and an intermediate field of 200 V cm^{-1}.

In simulating electron dynamics in the Monte Carlo simulator, we considered polar and non-polar acoustic phonon interactions, as well as polar and surface optical phonon interactions. Impurity and interface scattering rates are typically three orders of magnitude smaller and were hence neglected. Binary electron–electron scattering will only interchange two electrons in momentum space and hence not produce any change in the momentum of the ensemble as a whole. Thus, it will not cause the *ensemble-averaged* velocity to fluctuate in time. Consequently, it too is neglected. Since a major purpose of this work is to investigate the effect of acoustic phonon confinement on noise and velocity fluctuations, we have computed the relevant quantities using both bulk and confined acoustic phonon models. This allows us to compare the bulk and confined models.

3.1. The bulk acoustic phonon model

We first consider acoustic phonons as bulk modes. In figures 1 and 2, we show the temporal decay of the velocity autocorrelation function for the two different driving electric field strengths mentioned. The upper panel shows the results in the absence of any magnetic field and the lower panel shows the results in the presence of a transverse magnetic flux density of 10 T.

Looking at figure 1, it is obvious that the major effect of the magnetic field is to induce (decaying) oscillations in the autocorrelation function. These oscillations are a well-known signature of streaming in quasi-one-dimensional structures and arise when polar optical phonon scattering is the dominant energy relaxation mechanism. The autocorrelation function oscillates because an electron will be rapidly accelerated to the polar optical phonon emission threshold by the electric field, emit almost immediately, and fall to the bottom of the subband, repeating this process again and again. This oscillation in k-space (or energy space) leads to permanent oscillations in the velocity and mean energy *if* the entire ensemble is more or less in phase. When polar optical phonon scattering is overwhelmingly dominant, the ensemble remains in phase for a long time and the oscillations show up in the velocity autocorrelation function. This is a characteristic of 'streaming' transport and has been examined in references [3, 10, 11]. It should be noted that in a quantum wire, there is a singularity in the emission rate at the polar optical phonon energy because of the Van Hove singularity in the density of final states. This causes an almost impenetrable bottleneck at the phonon energy and makes streaming oscillations much more pronounced in quantum wires than in quantum wells and the bulk.

It is obvious that the phase of the oscillation will be randomized if there is significant

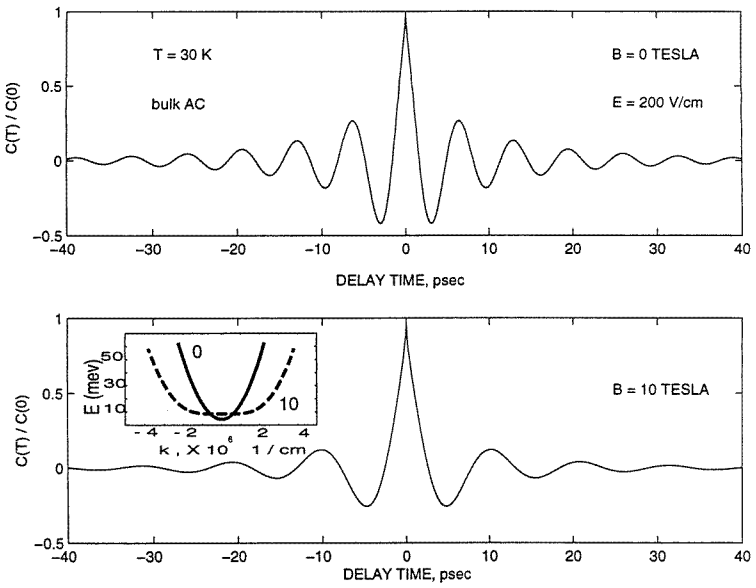

Figure 2. Temporal evolution of the velocity autocorrelation function at magnetic flux densities of 0 T (upper panel) and 10 T (lower panel). The driving electric field is 200 V cm^{-1} and the lattice temperature is 30 K. The electron temperature is 133 K at 0 T and 176.6 K at 10 T. A bulk acoustic phonon model has been assumed. The inset shows the electron's energy dispersion relation at magnetic flux densities of 0 and 10 T.

acoustic phonon scattering since that will randomly kick electrons out of phase with the rest of the ensemble. At a low driving electric field of 20 V cm^{-1}, acoustic phonon scattering usually dominates transport. Hence, the oscillations are ordinarily suppressed. However, a magnetic field brings out the oscillations because it quenches bulk acoustic phonon scattering [5] while increasing polar optical phonon scattering [12]. Thus, a magnetic field is conducive to streaming. Since the streaming oscillations will induce a peak in the noise spectral density, a magnetic field basically allows one to transfer noise energy from low frequencies to the higher-frequency peak by promoting streaming. Thus, it allows (in an appropriate context) beneficial 'noise engineering'.

Looking at figure 2, we find that streaming oscillations are much more pronounced when the driving electric field is 200 V cm^{-1}. At this intermediate electric field strength, polar optical phonon scattering is overwhelmingly dominant over acoustic phonon scattering and hence the electron ensemble streams in phase. A magnetic field increases the period of the oscillation. The oscillation period t_p is given by [7]

$$t_p = \frac{\overline{h}\,\Delta k}{eE} + \tau_{op} \tag{4}$$

where e is the electronic charge, E is the driving electric field, τ_{op} is the mean time that elapses after an electron crosses the polar optical phonon emission threshold and before it emits, and Δk is the change in the electron's wavevector (caused by the accelerating field E) during the free flight between two successive polar optical phonon scattering events.

In a magnetic field, the momentum p of an electron transforms according to $\vec{p}' = \vec{p} + e\vec{A}$ where $\vec{A}$ is the magnetic vector potential. As a result, the electron trajectories are elongated in k-space. Another way of viewing this is to look at the electron dispersion relations with and without a magnetic field as shown in the inset of figure 2. Obviously, in a magnetic field,

an electron's wavevector will have to increase more to gain the same amount of energy as in the absence of a magnetic field. Since Δk is larger in a magnetic field, the oscillation period increases.

We can check the validity of our picture with a simple comparison. If we assume that an electron scatters soon after it reaches the threshold for polar optical phonon emission and that such a scattering drops the electron down to near the bottom of the conduction band, then we can show that

$$t_p = \frac{\tau_{op}}{2} + \sqrt{\left(\frac{\tau_{op}}{2}\right)^2 + \frac{\sqrt{2m^*\hbar\omega_0}(\sqrt{2m^*\hbar\omega_0} + eE\tau_{op})}{e^2E^2}} \tag{5}$$

in the absence of any magnetic field (when the band structure is parabolic).

For $E = 200$ V cm^{-1}, the above equation yields a value of $t_p = 8$ ps ($\tau_{op} \approx 0$). The observed period in figure 2 ($B = 0$ T) is about 7 ps which is close enough to the estimated value to confirm that this simple picture originally presented in references [3,7,10,11] is quite reasonable.

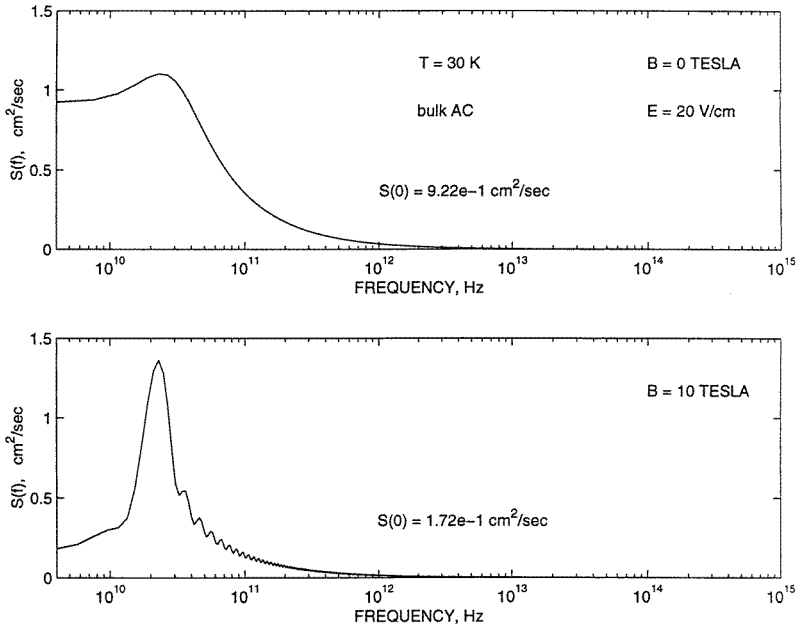

Figure 3. The spectral density of Johnson (or thermal) noise at magnetic flux densities of 0 T (upper panel) and 10 T (lower panel). The driving electric field is 20 V cm^{-1}. A bulk acoustic phonon model has been assumed.

In figures 3 and 4, we plot the Johnson noise spectral densities which are cosine transforms of the velocity autocorrelation functions. At a field strength of 20 V cm^{-1}, the spectral density in figure 3 has a very broad peak in the absence of any magnetic field, but a well-resolved narrower peak in a magnetic flux density of 10 T. Obviously, the well-resolved peak is caused by the magnetic field promoting carrier streaming. The rapid oscillations in the high-frequency tail of the spectral density (in a magnetic field) are just an artifact of the cosine transform algorithm and should not be taken as real.

In figure 4, which corresponds to a driving electric field of 200 V cm^{-1}, we see very well-resolved and narrow peaks associated with coherent streaming. A magnetic field red-shifts the

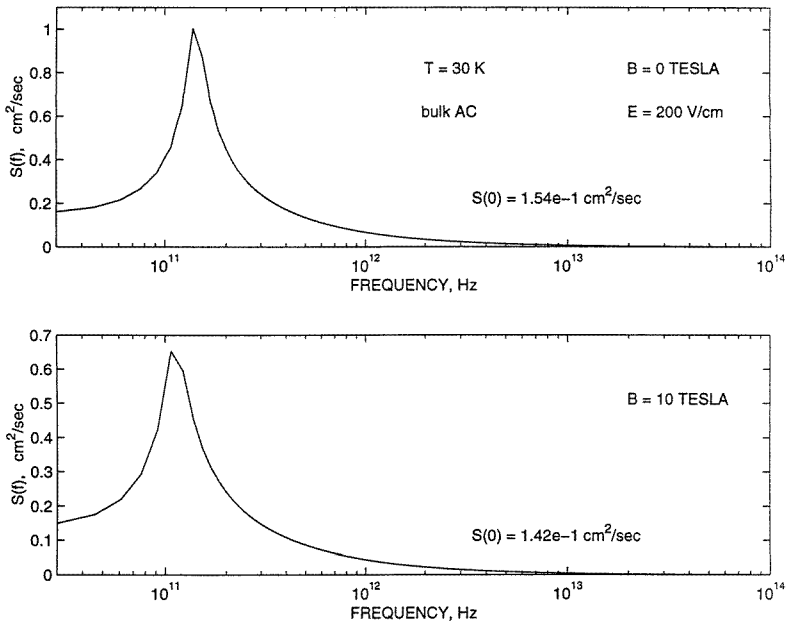

Figure 4. The spectral density of Johnson (or thermal) noise at magnetic flux densities of 0 T (upper panel) and 10 T (lower panel). The driving electric field is 200 V cm^{-1}. A bulk acoustic phonon model has been assumed.

peak slightly because it increases the period of the oscillations in the autocorrelation function as discussed before.

We point out that the correlation functions in figures 1 and 2 do not decay exponentially with time (since the scattering processes are not Markovian) and consequently the lineshapes of the noise spectral density peaks in figures 3 and 4 are not Lorentzian. As discussed before, this immediately makes the application of equation (3) suspect. Indeed, the diffusion coefficient calculated from equation (3) cannot be related to the mobility and electron temperature (found from the Monte Carlo simulation) by the Einstein relation—a point that we discuss later. Nonetheless, we have calculated an 'effective' diffusivity from equation (3) and examined its physical characteristics.

In figure 5, we show the dc component of this 'effective' diffusion coefficient $D(0)$ as a function of driving electric field at two different magnetic field strengths. The diffusion coefficient has a non-monotonic dependence on the electric field and has a broad peak. This feature is quite common in quantum wires and was also found in reference [3] where the peak was explained in terms of suppression of acoustic phonon scattering with increasing electric field. The final drop in the diffusivity is caused by the onset of streaming at higher electric fields [3].

In this paper, we have studied the effect of an external magnetic field on $D(0)$. A magnetic field decreases the diffusivity. Note that diffusivity is given by

$$D(0) = S(0)/4 = \int_0^\infty \mathrm{d}T\ C(T) \tag{6}$$

and hence it is the *area* under the autocorrelation function in figure 1 or 2. A magnetic field has two different effects. First, it decreases the decay rate of the autocorrelation function since it increases the momentum relaxation time by suppressing backscattering events [5]. This

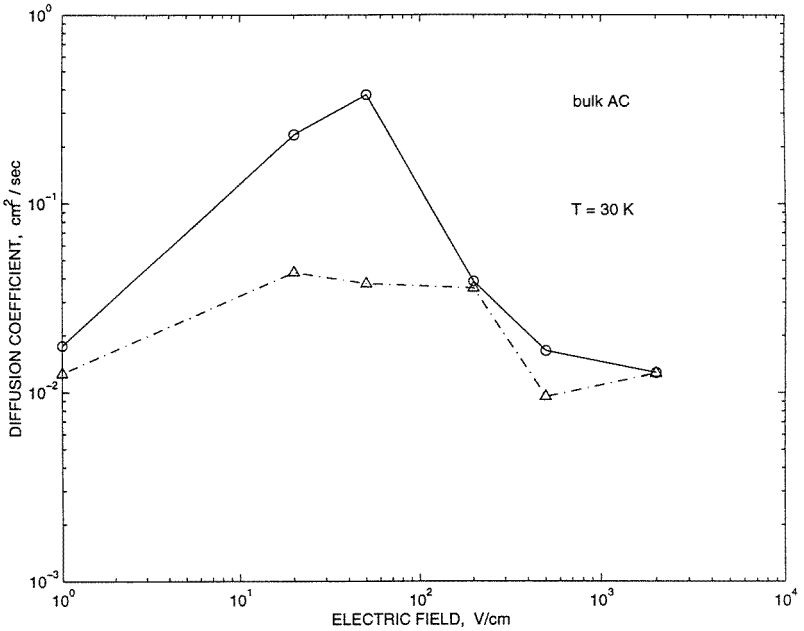

Figure 5. The diffusivity versus electric field at magnetic flux densities of 0 T (solid lines) and 10 T (broken lines). A bulk acoustic phonon model has been assumed.

tends to increase the area under the autocorrelation curve and thus increase the diffusivity. On the other hand, a magnetic field brings out oscillations in the autocorrelation function by promoting carrier streaming. This tends to reduce the area under the autocorrelation curve since the autocorrelation oscillates between positive and negative values. At the low and moderate electric field strengths that we consider in figure 5, the second effect is more important and hence the diffusivity is reduced by a magnetic field.

Table 1. Comparison of Wiener–Kintchine and Einstein diffusivities for the bulk phonon model.

Magnetic field (T)	Electric field (V cm^{-1})	Electron temperature (K)	Mobility (cm^2 V^{-1} s^{-1})	D_1 (cm^2 s^{-1})	D_2 (cm^2 s^{-1})
0	20	108	110000	0.22	516
10	20	108	140000	0.04	658
0	200	133.2	61500	0.38	350
10	200	176.6	44550	0.38	340

Let us compare the diffusivities obtained in figure 5 with those calculated from the Einstein relation. We will brand the diffusivity in figure 5 as the Wiener–Kintchine diffusivity and label it D_1 while that calculated from the Einstein relation is termed the Einstein diffusivity and labelled D_2. This comparison is shown in table 1.

Obviously, the two diffusivities are vastly different and this is because the existence of hot-electron effects gives the electron distribution function odd shapes in velocity space, with the result that $(1/2)m^*(v-v_d)^2 \neq kT_e$ where T_e is the electron temperature. Consequently, the Einstein relation is inapplicable. Second, the existence of non-Markovian scattering processes immediately makes equation (3) suspect. Price [15] has derived a different expression for the

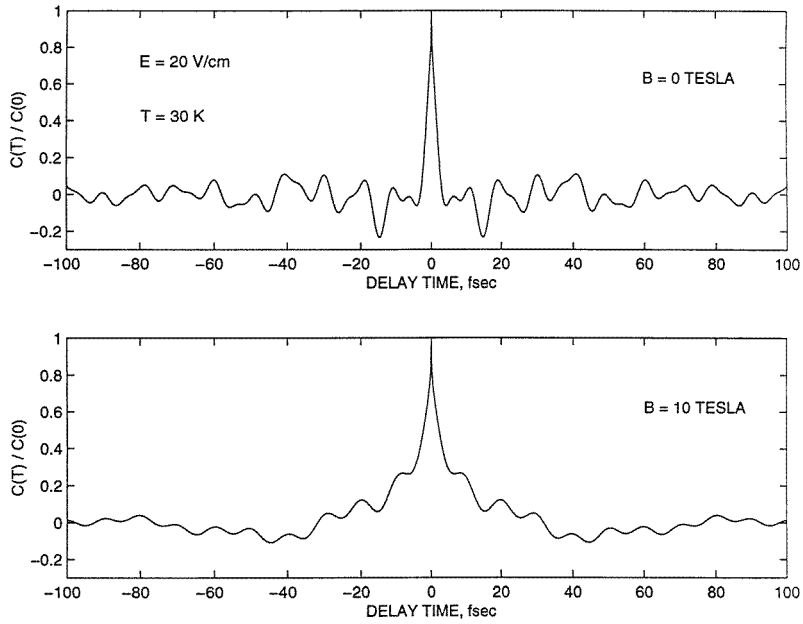

Figure 6. Temporal evolution of the velocity autocorrelation function at magnetic flux densities of 0 T (upper panel) and 10 T (lower panel). The driving electric field is 20 V cm^{-1} and the lattice (as well as the electron) temperature is 30 K. A confined acoustic phonon model has been assumed.

hot-carrier diffusivity which can be approximately written as

$$D_{\text{Price}} = \langle (v - v_d) v \tau \rangle \tag{7}$$

where v is the particle velocity, v_d is the drift velocity, and τ is the mean time between scattering events. The ensemble averaging denoted by $\langle\ \rangle$ is carried out over the carrier distribution function. If we heuristically assume that τ is constant and equal to the momentum relaxation time calculated from the dc mobility and moreover that $(1/2)m^*(v - v_d)^2 = kT_e$, then the Price diffusivity reduces to the Einstein diffusivity. However, in quantum wires, interactions are anisotropic and biased in favour of small-angle scatterings, so $\tau_m > \tau$. Furthermore, streaming (which orders the electron motion) tends to make $(1/2)m^*(v - v_d)^2 < kT_e$. Consequently, the Price diffusivity will certainly be less than the Einstein diffusivity and probably fall in between D_1 and D_2.

3.2. Confined acoustic phonons

In figures 6 and 7, we show the velocity and autocorrelation functions when acoustic phonons are treated as confined modes according to the prescription of reference [1, 2, 14]. There are rapid oscillations with multiple frequencies in the velocity autocorrelation function. These are caused by the same streaming effect, but this time the streaming agents are confined acoustic phonons with discrete energy rather than polar optical phonons. Since there are multiple phonon branches (and hence acoustic phonons with a plethora of frequencies), there are multiple periods of the oscillations. The periods of these oscillations are much smaller (see equation (2)) since the acoustic phonon energies are much smaller than polar optical phonon energies. A magnetic field appears to 'clean up' the oscillations somewhat since (i) it increases the period by elongating the electron trajectories in k-space, and (ii) the selection

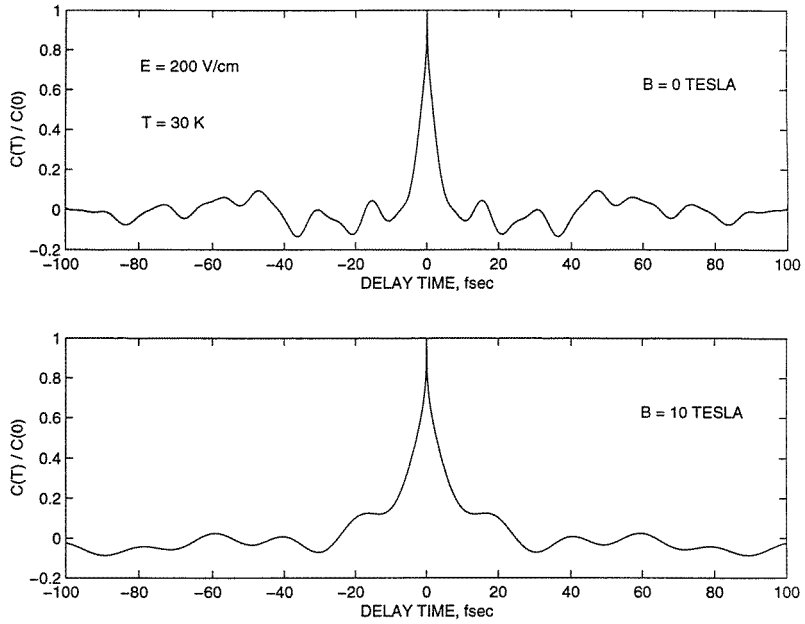

Figure 7. Temporal evolution of the velocity autocorrelation function at magnetic flux densities of 0 T (upper panel) and 10 T (lower panel). The driving electric field is 200 V cm^{-1} and the lattice (as well as the electron) temperature is 30 K. A confined acoustic phonon model has been assumed.

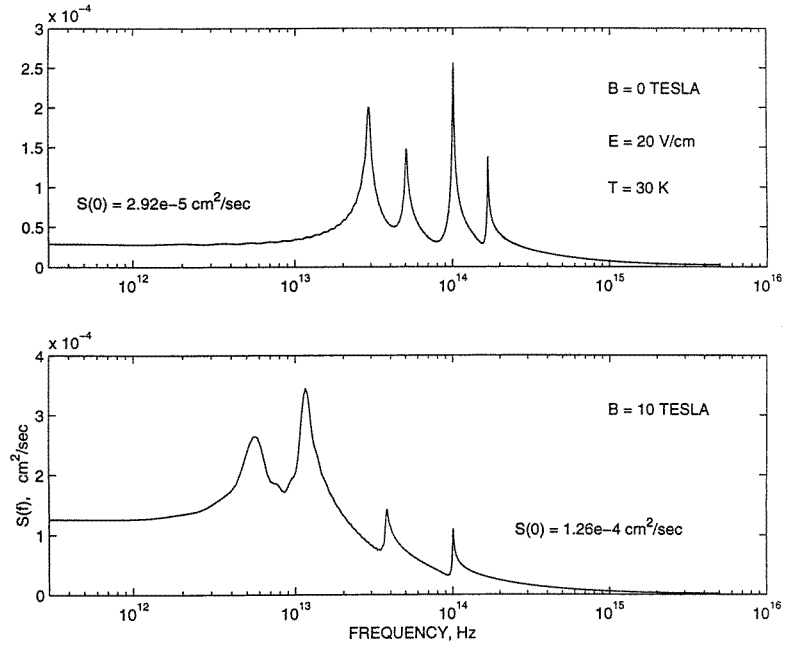

Figure 8. The spectral density of Johnson (or thermal) noise at magnetic flux densities of 0 T (upper panel) and 10 T (lower panel). The driving electric field is 20 V cm^{-1} and the lattice (as well as the electron) temperature is 30 K. A confined acoustic phonon model has been assumed.

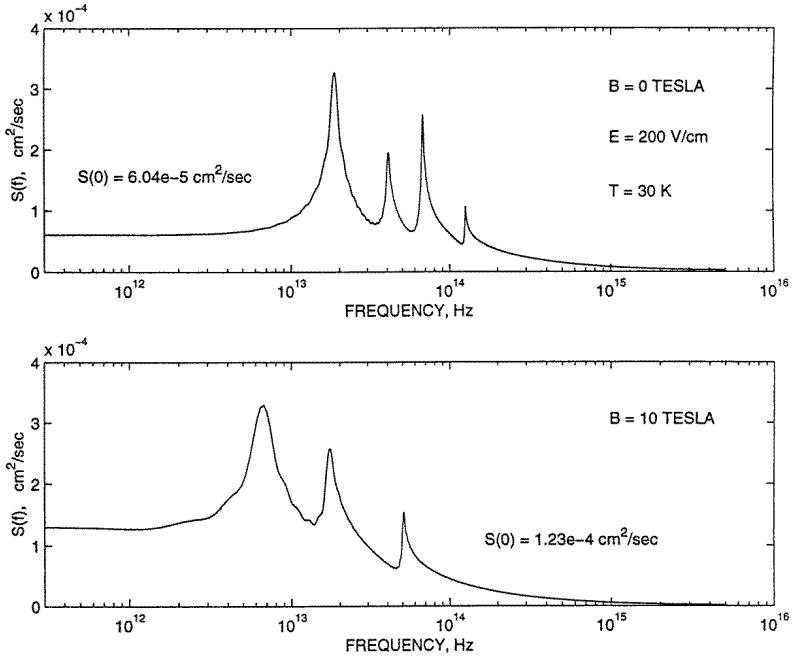

Figure 9. The spectral density of Johnson (or thermal) noise at magnetic flux densities of 0 T (upper panel) and 10 T (lower panel). The driving electric field is 200 V cm^{-1} and the lattice (as well as the electron) temperature is 30 K. A confined acoustic phonon model has been assumed.

rules for scattering (longitudinal momentum and energy conservation) are more restrictive in the presence of a magnetic field. Since backward scattering is strongly suppressed, only small momentum transfers via forward scattering are allowed. Thus, fewer phonon modes (which have small wavevectors and the correct energy) can participate in the scattering. As a result, there are fewer frequency components in the autocorrelation function.

In figures 8 and 9, we show the Johnson noise power spectrums. The infrared frequency peaks arise from the streaming oscillations in the velocity autocorrelation functions caused by *confined* acoustic phonon interactions. Thus, these peaks are a signature of acoustic phonon confinement. A magnetic field red-shifts the peaks since it increases the period of the streaming oscillations.

In figure 10, we plot the diffusivity as a function of electric field strength for two different magnetic fields. The difference between this figure and figure 5 is that here the acoustic phonons are treated as confined modes rather than bulk modes. Comparing this figure with figure 5, we find two major differences: (i) the diffusivity is lower by three orders of magnitude, and (ii) the dependence on the magnetic field is reversed. The first feature is caused by the fact that acoustic phonon confinement increases the electron–phonon scattering rate by several orders of magnitude [14]. This decreases the diffusivity. The second feature is caused by the fact that while a magnetic field reduces the decay rate of the velocity autocorrelation function (by suppressing backscattering) and thus increases the area under the autocorrelation curve, this is no longer offset by the fact that a magnetic field enhances oscillations in the autocorrelation function. In fact, the oscillations are there with or without a magnetic field. Thus, the area under the autocorrelation curve certainly increases in a magnetic field and this increases the diffusivity. As a result, the magnetic field dependence of the diffusivity shows

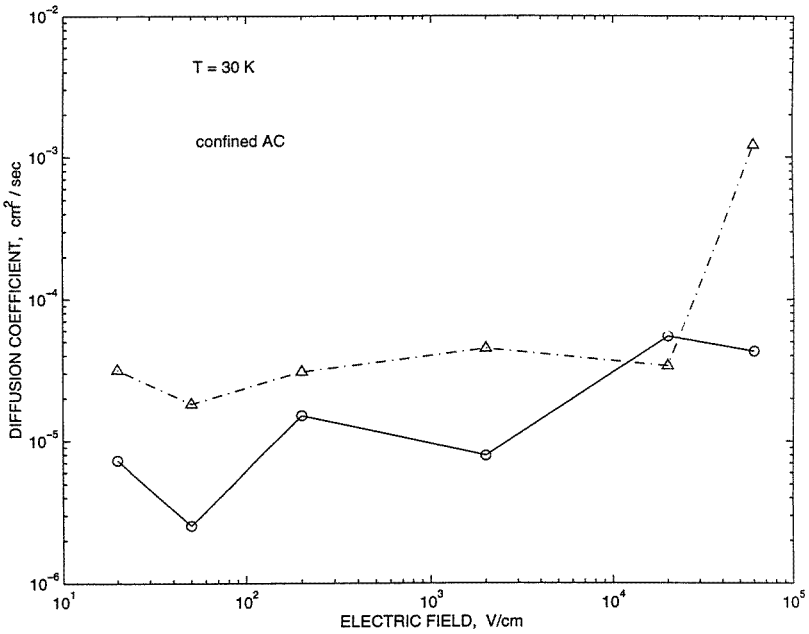

Figure 10. The diffusivity versus electric field at magnetic flux densities of 0 T (solid lines) and 10 T (broken lines). A confined acoustic phonon model has been assumed.

opposite behaviours in figures 5 and 10.

We will once again compare the Wiener–Kintchine diffusivity and the Einstein diffusivity as we did in the case of the bulk phonon model. This comparison is shown in table 2. Again, we observe the same trend as in the case of the bulk phonon model.

Table 2. Comparison of Wiener–Kintchine and Einstein diffusivities for the confined phonon model.

Magnetic field (T)	Electric field (V cm^{-1})	Electron temperature (K)	Mobility (cm^2 V^{-1} s^{-1})	D_1 (cm^2 s^{-1})	D_2 (cm^2 s^{-1})
0	20	30	375	8×10^{-6}	0.975
10	20	30	215	22×10^{-6}	0.559
0	200	30	88.5	12×10^{-6}	0.23
10	200	30	159	18×10^{-6}	0.413

Before concluding, we point out two additional features. The extremely strong coupling of electrons to *confined* acoustic phonons causes the diffusivity to plummet, resulting in mean free paths on the order of 1 nm. Such mean free paths are observed in dirty metals on which a large number of mesoscopic experiments have been carried out [16]. However, in those systems, the mean free path is determined primarily by elastic scatterings which do not randomize an electron's phase. Hence the phase-breaking length is much larger than 1 nm. However, in our case, the mean free path is determined entirely by phase-breaking inelastic scatterings resulting in phase-breaking lengths of $\sim$1 nm. Hence, phonon confinement has a very deleterious effect on phase coherence; one would not use free-standing quantum wires for quantum interference experiments. The high phonon scattering rate also explains why the electron temperature is equal to the lattice temperature even at 30 K. The extremely high confined acoustic phonon

emission rate quickly equilibriates the electron population with the lattice, thus precluding any serious non-equilibrium phenomena.

4. Conclusions

In this paper, we have shown the effects of acoustic phonon confinement on Johnson noise and carrier diffusivity in a free-standing quantum wire. Since it is generally very difficult to demonstrate unambiguously acoustic phonon confinement in quantum structures, the appearance of new noise peaks at well-separated frequencies and a drastic reduction of carrier diffusivity that are caused by acoustic phonon confinement provide an important diagnostic technique for monitoring the existence and dominance of phonon confinement. Of course, it is understood that measurement of noise power spectra at infrared frequencies is a very 'tall order' and may stretch beyond current state of the art. However, future developments in this direction may allow it to happen. Thus, we believe that these results will find applications in the experimental study of carrier transport in low-dimensional systems.

Acknowledgment

This work was partly supported by the US Army Research Office under a short-term analytical-services agreement.

References

[1] Svizhenko A, Bandyopadhyay S and Stroscio M A 1998 *J. Phys.: Condens. Matter* **10** 6091
[2] Svizhenko A, Balandin A, Bandyopadhyay S and Stroscio M A 1998 *Phys. Rev.* B **57** 4687
[3] Mickevicius R, Mitin V V, Harithsa U K, Jovanovic D and Leburton J P 1994 *J. Appl. Phys.* **75** 973
[4] Lundstrom M S 1990 *Fundamentals of Carrier Transport (Modular Series on Solid State Devices vol 10)* 1st edn (Reading, MA: Addison-Wesley) ch 3, pp 118–22
[5] Telang N and Bandyopadhyay S 1993 *Appl. Phys. Lett.* **62** 3161
[6] Chaudhuri S and Bandyopadhyay S 1992 *J. Appl. Phys.* **71** 3027
[7] Briggs S and Leburton J P 1988 *Phys. Rev.* B **38** 8163
[8] Jovanovic D and Leburton J P 1991 *Monte Carlo Device Simulation: Full Band and Beyond* ed K Hess (Boston, MA: Kluwer–Academic) pp 191–218
[9] Telang N and Bandyopadhyay S 1995 *Phys. Rev.* B **51** 9728
[10] Jovanovich D and Leburton J P 1992 *Superlatt. Microstruct.* **11** 141
[11] Mitin V and VanVliet C M 1990 *Phys. Rev.* B **41** 5332
[12] Telang N and Bandyopadhyay S 1993 *Phys. Rev.* B **48** 18 002
[13] Poborchii V V, Ivanova M S and Salamatina I A 1994 *Superlatt. Microstruct.* **16** 133
[14] Yu SeGi, Kim K W, Stroscio M A, Iafrate G J and Ballato A 1994 *Phys. Rev.* B **50** 1733
[15] Price P J 1965 *Fluctuation Phenomena in Solids* ed R E Burgess (New York: Academic) pp 355–80
[16] See, for example, Beenakker C W J and van Houten H 1991 *Solid State Physics* vol 44, ed H Ehrenreich and D Turnbull (San Diego, CA: Academic)